Chapter 8
Radiology in TB Spine (X-rays, Ultrasound, CT, MRI)

Anindita Sinha, Stanzin Spalkit, Anuj Prabhakar, and Mahesh Prakash

Abstract Spine is the most common site of skeletal involvement by tuberculosis (TB). Imaging plays an important role in its diagnosis, deciding management strategies, detects and predicts complications and monitors response to therapy. Out of the different modalities available,

The paradiscal, central, anterior subligamentous and neural arch are the common patterns of vertebral involvement. Thoracolumbar junction is the most common site of involvement. Plain radiographs are usually the initial investigation in spinal TB. A minimum of 30% bone mineral loss is required for the lesion to be conspicuous on a plain radiograph. Computed tomographic scanning provides better bony detail and delineation of the pattern of bone destruction, especially in areas that are inaccessible to evaluation by plain X-ray. Its major role lies in the detection of subtle calcification in the paraspinal collection as well as in providing guidance for targeted aspiration or biopsy. Magnetic resonance imaging (MRI) is the modality of choice for Pott's spine and is more sensitive as well as specific than other modalities. MRI demonstrates involvement of all the components of the spine, including vertebral body, intervertebral disc, the posterior elements, epidural extension of disease and the spinal cord involvement. The exact extent of paraspinal granulation tissue and collection is demarcated well on MRI. It also has a crucial role in post-treatment response assessment besides detection of complications.

Keywords Tuberculosis · Spine · MRI · Radiograph · Vertebra · Central · Paradiscal · Subligamentous · Neural

India accounts for 23% of the worldwide TB burden [1]. Around 10% of the extrapulmonary TB are contributed by skeletal TB, with spinal TB being the most common site of involvement [2].

A. Sinha (✉) · S. Spalkit · A. Prabhakar · M. Prakash
Department of Radiodiagnosis, Post Graduate Institute of Medical Education & Research, Chandigarh, India
e-mail: Official-sinha.anindita@pgimer.edu.in

S. S. Dhatt, V. Kumar (eds.), *Tuberculosis of the Spine*,
https://doi.org/10.1007/978-981-16-9495-0_8

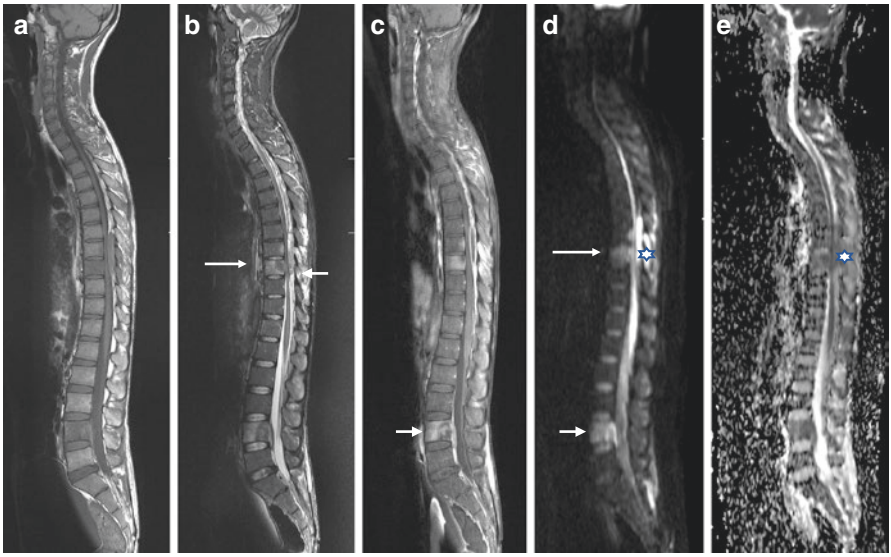

Fig. 8.1 Sagittal T1 (**a**), T2 (**b**), T1 post-contrast (**c**), DWI (**d**) and (**e**) ADC images of the whole spine in a case of multifocal caries spine reveal T1 hypointensity, T2 hyperintensity, post-contrast enhancement and diffusion restriction involving D8, D9 vertebral body (arrow) with an epidural peripherally enhancing collection (empty arrow) and posterior spinous process involvement from D7 to D9 level (asterix). Similar vertebral involvement also seen at L4 level (small arrow). A small epidural component is also seen at this level

Plain radiographs may be normal in early disease. A 30% mineral loss must occur before the lesions become conspicuous radiographically. An average of 3.4 to 3.8 vertebral involvement has been reported by various authors over the years [3, 4]. Extensive vertebral involvement may be seen in immunocompromised state, diabetics and hemoglobinopathies.

'Skipped lesion' where two non-contiguous vertebrae are involved without the involvement of intervening vertebral bodies and intervertebral discs are seen in 7% of the cases; the spread of infection along the Batson's perivertebral plexus of veins is proposed to be the mechanism (Fig. 8.1) [5].

Most common site of involvement is dorsal spine followed by the lumbar region. The vertebral body is more frequently affected than the posterior arch.

Four distinct radiological types of vertebral involvement have been described: paradiscal (most common), anterior, central, neural arch or appendiceal (pedicles, laminae, spinous process or transverse processes) [6].

8.1 Paradiscal Type

It is the most common pattern of vertebral involvement where simultaneous involvement of two contiguous vertebrae adjacent to the disc space is seen. This suggests a common blood supply to this region. On radiographs, it is manifested as reduction

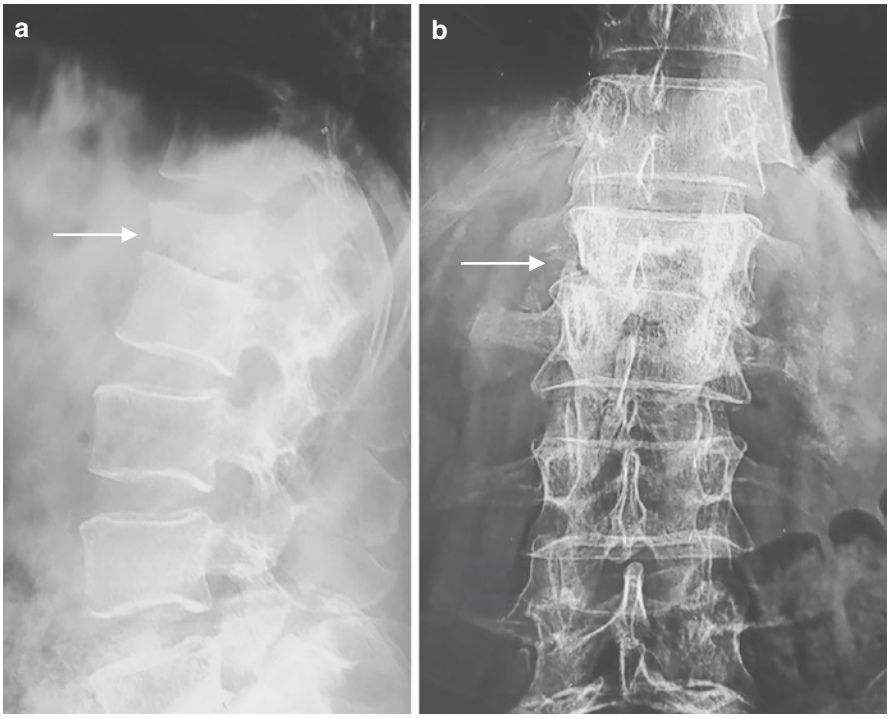

Fig. 8.2 Radiograph lateral (**a**) and AP (**b**) view reveal loss of intervertebral disc space associated with destruction of the anteroinferior aspect of L1 vertebral body (arrow)—*marginal variety of caries*

in intervertebral disc space associated with irregularity of endplates in the adjacent vertebrae (Figs. 8.2 and 8.3) [7].

Paravertebral shadow: Tuberculous granulation tissue as well as abscess formation in the paravertebral region is seen on plain radiographs in the form of soft tissue shadows adjacent to the spine. In the cervical region, it is best seen on a lateral radiograph as increased prevertebral soft tissue shadow [8]. The normal space between the vertebral bodies and pharyngeal/tracheal shadow measures approximately 5 mm above the cricoid cartilage level and 15 mm below this level. Anteroposterior diameter of the prevertebral soft tissue shadow should not exceed that of the adjacent vertebral bodies [9].

In the upper dorsal spine region (from the C7 to D4 region), it may manifest on an AP view as widening of the superior mediastinum**.** A good quality X-ray may help in early diagnosis in this region. In the lateral view, the contour of the posterior tracheal wall should be looked for, which normally appear concave anteriorly [7]. Any change in the normal contour (anterior convexity of the tracheal shadow) and/or a distance >8 mm from the vertebrae should prompt a search for vertebral disease from C7 to D4 level. Abscesses below the D4 vertebral level produce typical fusiform-shape (bird nest appearance), a larger sized abscess may produce a broad

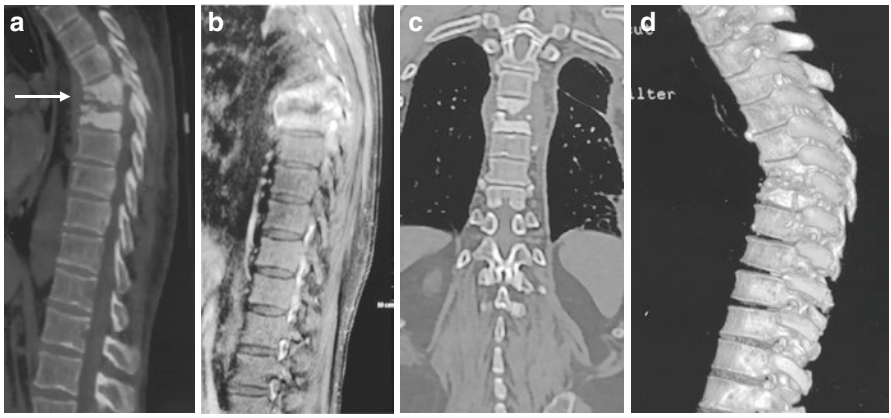

Fig. 8.3 CT spine sagittal (**a**), coronal CT (**c**) and virtual reconstructed 3D image (**d**) reveals loss of D4/5 intervertebral disc space with simultaneous destruction of the adjacent contiguous vertebrae (D4 and D5) causing a focal kyphotic deformity (arrow). T1 weighted post-contrast sagittal image (**b**) showing the paradiscal involvement of the D4 and D5 vertebrae with intervening disc involvement

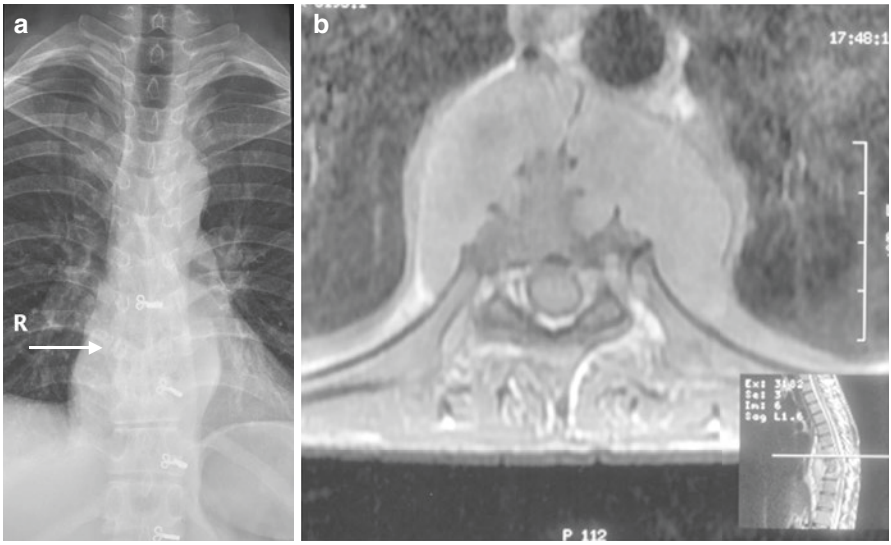

Fig. 8.4 Chest X-ray PA view (**a**) of a patient with tuberculosis D8–10 vertebrae seen as a retrocardiac shadow.(arrow) Axial T1 weighted MRI (**b**) of the same patient reveals a pre and paravertebral abscess at D8 level

posterior mediastinal shadow. (Fig. 8.4) An abscess under tension may give rise to a globular-shaped shadow. In the lumbar region, abscess tracking along the psoas muscle appear as widening of the psoas shadow.

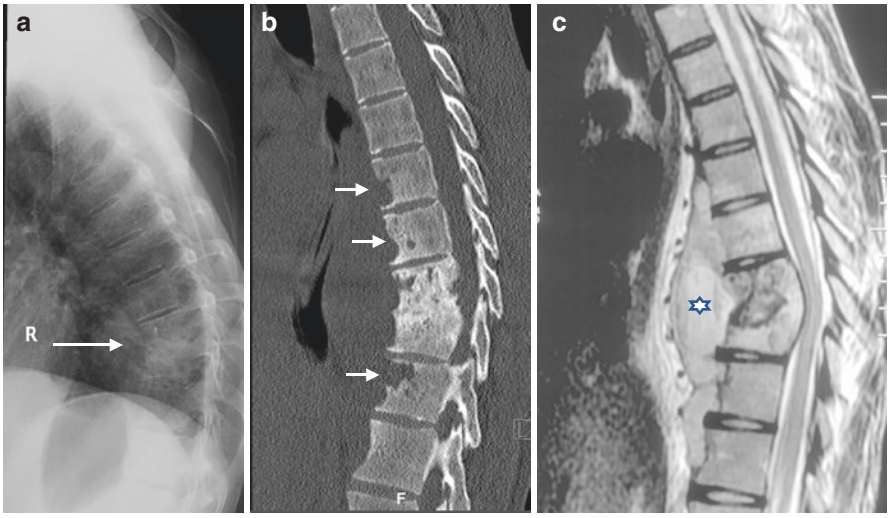

Fig. 8.5 X-ray lateral view DL spine (**a**) showing loss of D9/10 disc space with adjacent vertebral destruction with focal kyphosis (arrow), NCCT spine sagittal view (**b**) additionally shows destruction along the anterior aspect of D7,D8 and D11 (short arrow) with relative preservation of the disc spaces at these levels giving the 'saw tooth appearance' along with large prevertebral soft tissue. T2 weighted MRI sagittal view (**c**) reveals the large subperiosteal collection deep to Anterior Longitudinal Ligament (ALL) (asterix) with destruction of adjacent anterior vertebral cortices besides the paradiscal destruction at D9/10 level

An absence of osseous disease in the presence of a large paraspinal abscess may be identified rarely at radiography. CT may help demonstrate a small focus of vertebral involvement. Small perivertebral abscess may not be visible on radiography [10].

An 'aneurysmal phenomenon' is described where a paravertebral abscess remains under tension for a long time and causes erosion along the anterior margin of the vertebral bodies with sparing of the intervertebral discs because of its elasticity giving rise to the 'saw tooth' appearance [11] (Fig. 8.5).

Calcification within an abscess is pathognomonic of spinal tuberculosis. It is proposed to occur due to lack of proteolytic enzymes in *Mycobacterium tuberculosis*. Plain X-rays are superior to MRI for the evaluation of calcification [12] (Fig. 8.6).

Deformity: In long-standing cases, contiguous paradiscal vertebral bodies are destroyed, and one or both bodies show wedge collapse and angulation of spine with convexity posteriorly. Involvement of the dorsal vertebrae leads to a kyphotic deformity which is the most common spinal deformity (Fig. 8.3). Involvement of multiple adjacent vertebrae may result in a severe kyphotic deformity [13].

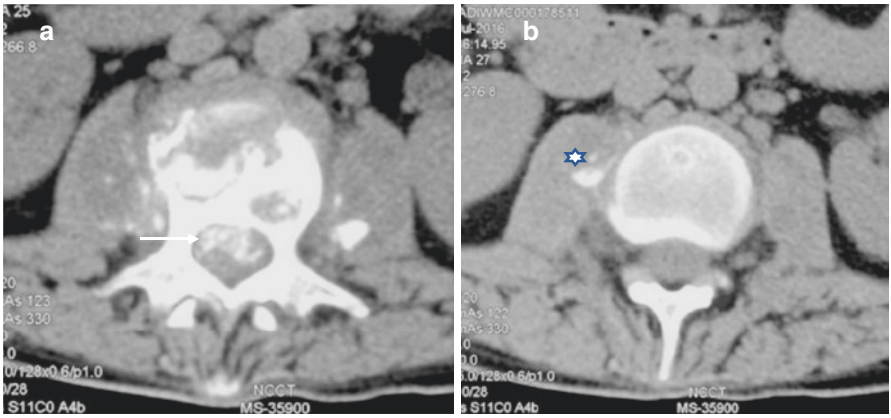

Fig. 8.6 NCCT Axial section (**a**) through the lumbar region reveals fragmentary vertebral destruction with associated paravertebral collection showing calcification within. Destroyed bone fragments are also seen in the epidural space (arrow). Axial CT section at a lower level (**b**) showing a right psoas abscess with few specks of calcification (asterix)

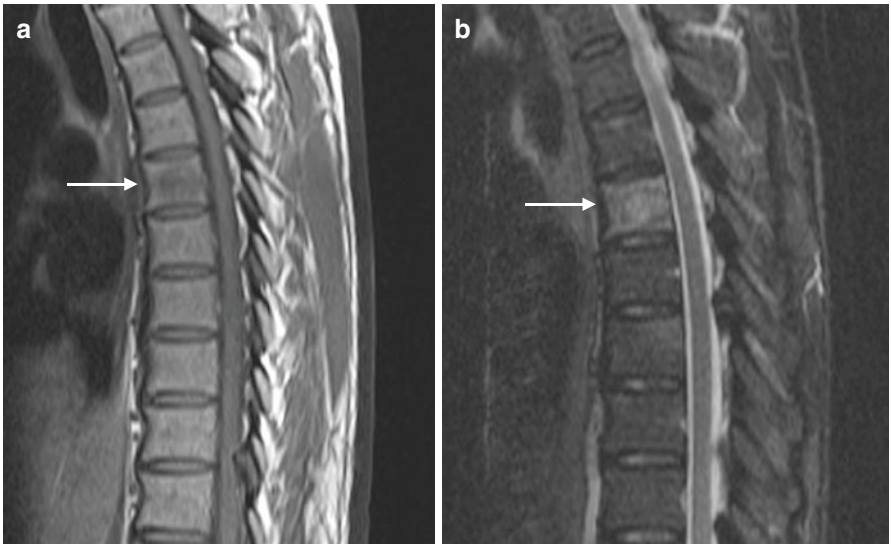

Fig. 8.7 Sagittal T1 (**a**) and fat-suppressed T2 weighted (**b**), post-contrast images showing altered signal intensity within the vertebral body (arrow) (T1 hypointensity and T2 hyperintensity) with preserved cortices and discs

8.2 Central Type

This pattern of involvement arises when the infection starts from the centre of the vertebral body when the bacteria inseminates through Batson's venous plexus or via the posterior vertebral artery branches (Fig. 8.7). Later, due to loss of trabeculae

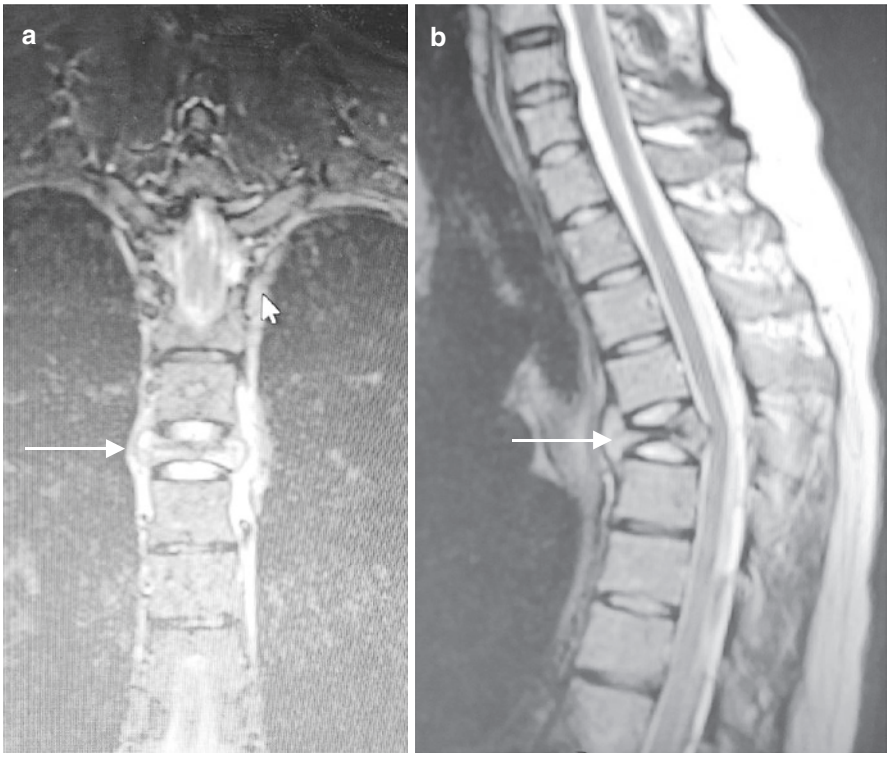

Fig. 8.8 T2 weighted coronal (**a**) and sagittal (**b**) images showing D5 complete collapse (arrow) with a small pre and paravertebral collection. Note the sparing of the contiguous discs

there is collapse of the diseased vertebral body on axial loading [5]. In contrast to the paradiscal type, loss of disc space and paravertebral shadow is minimal, hence, it is often confused with neoplastic aetiology (Fig. 8.8). However with longer follow up, diminution of adjacent disc space may be observed [14].

8.3 Anterior Type

This pattern is seen when disease process begins just deep to the anterior longitudinal ligament and periosteum (Fig. 8.5). This causes erosions of the anterior aspect of vertebral body, which is seen on lateral radiographs as irregular cortical margins. With extension of the disease underneath the anterior or posterior longitudinal ligaments, there may be involvement of multiple contiguous vertebrae. Vertebral body collapse with diminution of adjacent disc space is usually minimal and is seen at a later stage [5].

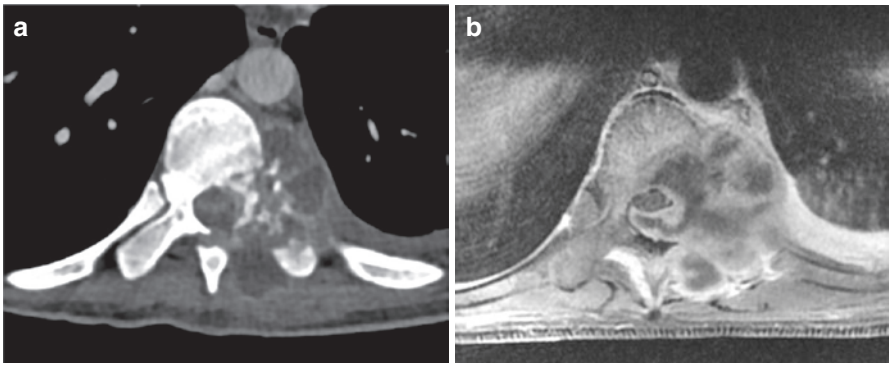

Fig. 8.9 Axial CT (**a**) sections soft tissue window showing lytic lesions involving the left pedicle, adjacent lamina and posterior body of dorsal vertebra. On axial T1 post-contrast study (**b**: associated soft tissue extending into the spinal canal is also seen—Neural arch tuberculosis

8.4 Appendiceal Type

This includes involvement of the neural arch (pedicles and laminae), transverse processes and spinous process either in isolation or combined (Fig. 8.9). Radiographically, these lesions may be suspected when indirect signs of involvement are seen, such as paravertebral shadows or erosive changes with an intact disc [15]. The involvement of posterior spinal joints is difficult to appreciate on routine radiography [16]. Posterior spinal articulations may also be involved and give rise to a rare deformity called lateral translation in addition to the more common paradiscal lesions [17].

The main disadvantage of radiographs is its low sensitivity in the early stages of the disease. Vertebral sites that are difficult to assess on X-ray include craniovertebral and cervicodorsal junction [18]. Assessment of spinal cord changes, involvement of soft tissue, exact site and extent of abscesses is difficult to decipher on plain X-rays. Hence, visualization of any of the radiographic signs may indirectly mean that the disease process has reached a relatively advanced stage [19, 20].

Simultaneous presence of pulmonary tuberculosis is common in patients with spinal tuberculosis. A primary focus in the lung or a history of pulmonary tuberculosis can be obtained in 67% of patients spinal tuberculosis [21].

Ultrasound can help diagnose the presence of tubercular abscesses, assess the nature (solid or fluid) of iliopsoas mass and quantify the drainable content especially in lumbar vertebral disease.

8.5 Computed Tomography

Findings are conspicuous much earlier on CT than plain radiography as it demonstrates better detail of bony irregularity/disruption, sclerosis and disc collapse. Various patterns of bone destruction have been described; fragmentary (Figs. 8.10,

Fig. 8.10 Axial NCCT section through the dorsal vertebral body showing gross destruction of bone with numerous residual small bone fragments

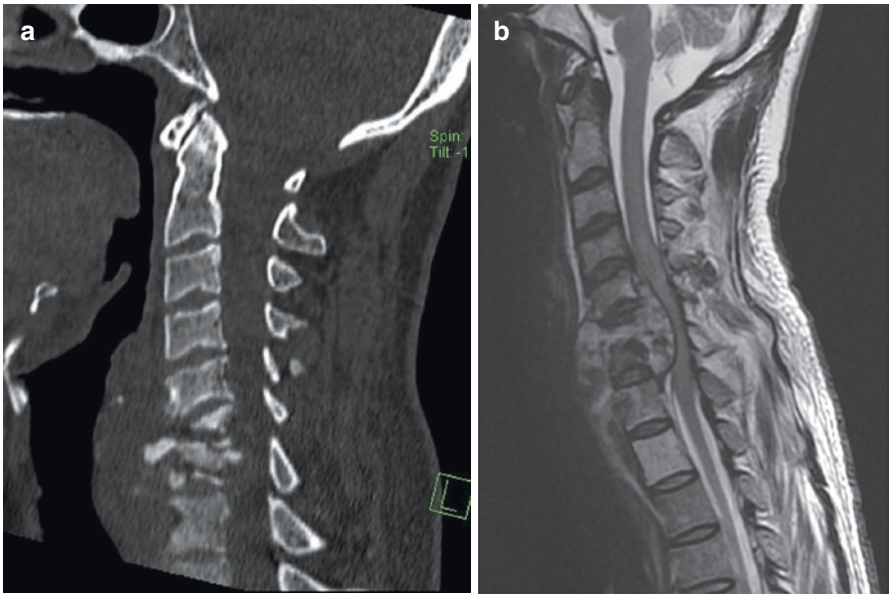

Fig. 8.11 Sagittal NCCT (**a**) and T2W images (**b**) cervical spine MR scans of a patient with tuberculosis of C5–7 show fragmentary destruction and collapse of C6 and C7 vertebral body with the destruction of the intervening disk space. A prevertebral abscess lifting up the anterior longitudinal ligament and a small ventral epidural collection are also seen

and 8.11), osteolytic, sclerotic and subperiosteal (Fig. 8.5). Besides bony detail, paraspinal abscesses are also better evaluated than plain radiography. It has a crucial role in demonstration of calcification within an abscess or bone fragments within epidural lesions (Fig. 8.6). It is of great value in providing guidance for percutaneous diagnostic sampling, especially in inaccessible sites. The major disadvantage is in evaluation of effect of the disease on neural structures for which MRI scores over CT.

Radiological evidence of healing lags behind the clinical and laboratory findings in spinal tuberculosis. X-rays or MRI done after few months after the start of multi-drug therapy may not show any signs of improvement in many patients and should not be labelled as treatment failure. However, if the images do not show improvement when repeated more than 6 months after the onset of treatment, one should consider the possibility of an alternative pathology or a therapeutically refractory disease. Once the disease has healed, the bony architecture is restored. Rarely the healing is accompanied by fat replacement of the healed area.

8.6 MRI

MRI scores over other imaging modalities with its superior soft tissue contrast and its ability to detect and delineate changes in the marrow, the intervertebral disc and the spinal cord [6].

MRI is the modality of choice for the overall evaluation of tuberculous spine. It has a special role in the evaluation of disease in difficult sites like craniovertebral junction (Fig. 8.12), cervicodorsal junction, neural arch elements and vertebral appendages, the sacroiliac joint region (Fig. 8.13), sacrum and coccyx.

Fig. 8.12 Lateral view cervical spine show increased atlanto-dental interval and indistinct cortical margins of the odontoid process, subtle amorphous calcification is seen anterior to the D2 body (arrow)

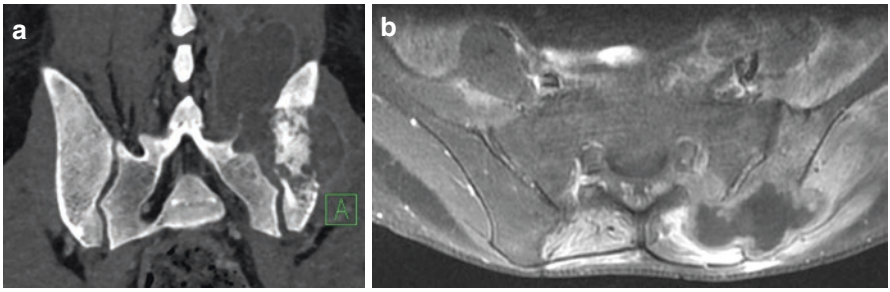

Fig. 8.13 (**a**). CT through the sacroiliac (SI) joint reveal left iliac bone destruction with periarticular fluid collection (**b**) Axial T1 weighted post-contrast image MRI image of the same patient showing abnormal enhancement and destruction of the left iliac bone with peripherally enhancing collection in posterior aspect of the left SI joint

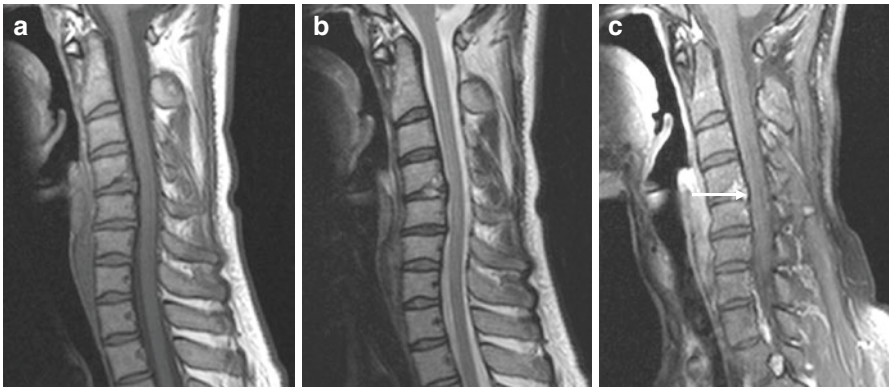

Fig. 8.14 Sagittal T1(**a**), T2(**b**) weighted and post-contrast T1 (**c**) weighted images showing altered signal within C4/5 intervertebral disc which appears T2 hyperintense and show post-contrast enhancement in the posterior aspect s/o discitis (arrow). There is endplate irregularity with enhancement of inferior sub endplate region of C4 vertebral body -spondylodiscitis

Usual MRI protocol includes non-contrast T1-weighted (T1W), T2-weighted (T2W) and short tau inversion recovery (STIR) sequences in axial, sagittal and coronal planes along with contrast-enhanced T1W fat-suppressed sequences after gadolinium contrast injection.

MRI appearances can be described according to the phase or activity of the disease process.

In the Active Stage: The vertebral body involvement is seen as abnormal marrow signal intensity, which appears hypointense on T1W and hyperintense on T2W sequences showing heterogeneous enhancement associated with loss of cortical definition [16, 22] (Fig. 8.14). Contiguous vertebral body disease with disc destruction (osteitis and discitis) is common. Disc involvement manifests as loss of normal internuclear cleft with increased signal on T2-weighted images and post-contrast

enhancement. Due to the lack of proteolytic enzymes in mycobacterium, disc involvement occurs relatively late compared to pyogenic spondylitis. The 'floating disc sign' may appear rarely if there is significant vertebral destruction with sparing of the disc. In paediatric cases, the disc is well hydrated and is more prone for infection [23].

Abscess formation in and around the vertebral lesion is a characteristic feature of spinal tuberculosis, with occurrence of prevertebral, paravertebral and epidural masses seen in approximately 71% of the cases on MRI [23] (Fig. 8.15). MRI is highly accurate in distinguishing granulation tissue from abscess. Both granulation tissue and abscess appear hypointense on T1 and hyperintense on T2; however, on post-contrast study an abscess reveals thick rim enhancement while a granulation tissue or phlegmon reveals more uniform enhancement [16, 22, 23] (Figs. 8.15 and 8.16). In thoracic

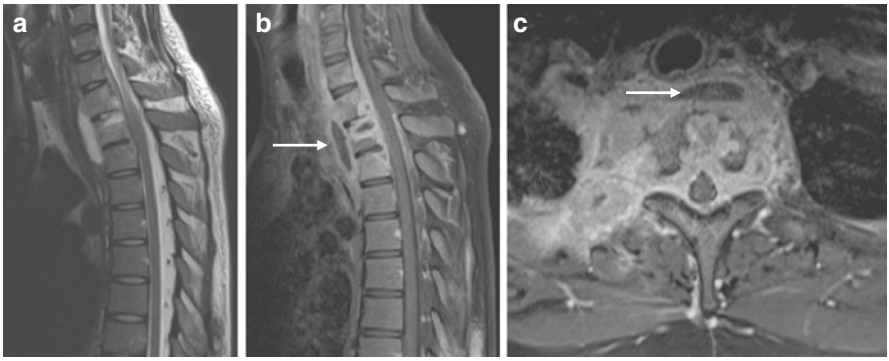

Fig. 8.15 Sagittal T2 weighted (**a**), T1 post-contrast sagittal (**b**) and axial (**c**) images show altered signal with enhancement of multiple contiguous upper dorsal vertebrae with associated prevertebral collection with thick peripheral enhancement (arrow) suggestive of abscess with homogenously enhancing paravertebral granulation tissue in right paravertebral area. Extradural extension of the granulation tissue circumferentially around the spinal cord is seen

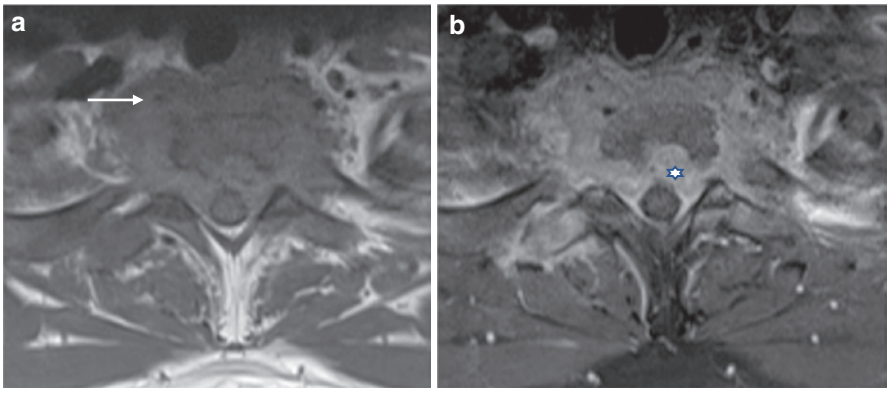

Fig. 8.16 Axial T1 non-contrast (**a**) and T1 post-contrast (**b**) scan of the same patient as in Fig. 8.15 show T1 isointense and homogenous post-contrast enhancement within the pre and paravertebral tissue (arrow). A ventral epidural extension is also seen (asterix)

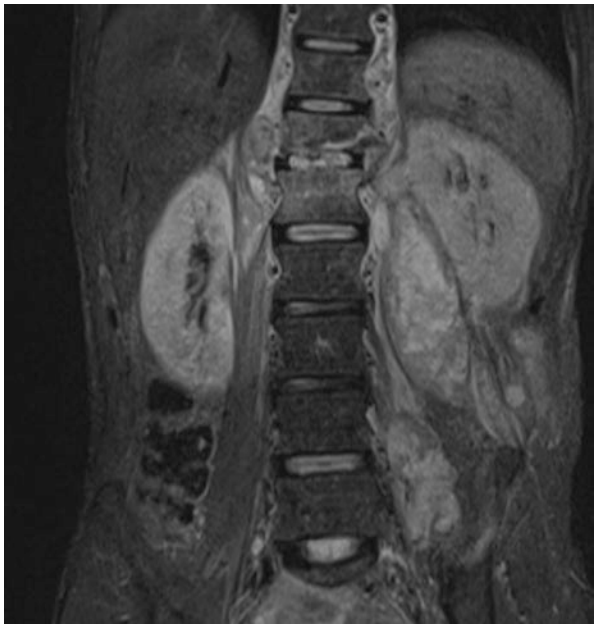

Fig. 8.17 T1 post-contrast coronal scan in a patient with dorso-lumbar TB spine depicts partial collapse of D12 and enhancement of D12 and L1 vertebrae. There is a disproportionately large psoas abscess on the left side posterosuperiorly displacing the left kidney

region, the paraspinal collection can extend along the intercostal space or track into the mediastinum or pleural cavity, or rarley encase the intercostal arteries as they barely penetrate the anterior longitudinal ligament [24]. In the lumbar region, in case of psoas muscle involvement, there is loss of normal muscle morphology, increase muscle bulk with uniform signal intensity on T1W images. On T2W images, the psoas abscess is seen as high signal fluid with thick peripheral post-contrast enhancement (Fig. 8.17).

The following MRI features show high sensitivity and specificity for spinal tuberculosis: end plate disruption, 100 and 81.4%, respectively, paravertebral soft tissue shadow (96.8%, 85.3%) and an increased T2 signal intensity of intervertebral disk (80.6%, 82.4%) [25].

Posterior element involvement is rare in tuberculosis, however, it is more common than in pyogenic infection. Involvement by the disease manifests as abnormal signal and inhomogeneous enhancement of the affected site. The posterior elements may be affected in isolation (Fig. 8.18), however, more commonly they are seen in combination with the anterior element lesions. Combined involvement of the posterior and anterior elements is referred to as ‘composite lesions or pan vertebral lesion’ [26]. There may be associated granulomatous lesions within the spinal canal either with involvement of epidural/subdural space or that of spinal cord. Epidural extension is detected by MRI in about 61% of involved vertebrae [23]. Compressive myelopathy may result due to compression of the spinal cord from posterior aspect [27–29] or from anterior aspect [30] (Fig. 8.11).

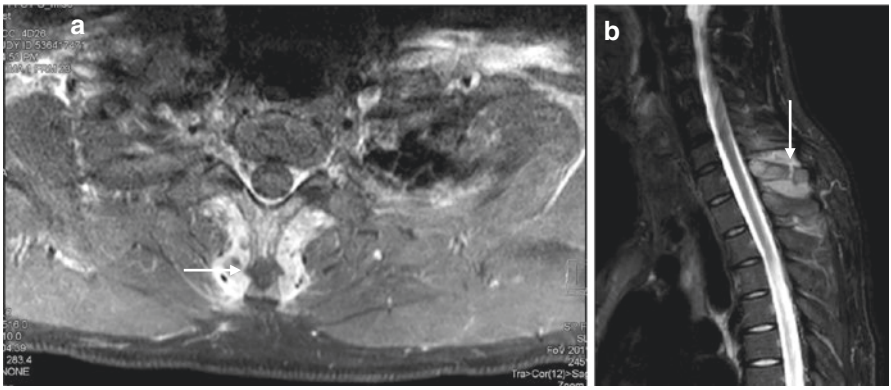

Fig. 8.18 Post-contrast T1W axial MR (**a**) and sagittalT2 weighted image (**b**) of a patient with TB spine showing T2 hyperintensity and abnormal enhancement of the spinous process of C6 vertebra with an undisplaced fracture line through it (arrow in **b**). There is surrounding homogenous enhancement

8.7 Cord Changes

Neurological deficit due to involvement of posterior element by tuberculosis is not uncommon [1, 17]. Common causes include extrinsic mechanical compression on the cord by abscesses, granulation tissue or debris, internal gibbus and subluxation. It is rarely due to direct involvement of the cord by the disease process as the cord can withstand slowly developing pressure exerted over a long period of time due to relatively high physiologic reserve, such that even a significant reduction in cord diameter is compatible with good cord function. Most patients present with compression paraplegia rather than sensory deficit, this is because motor fibres are more susceptible to pressure effect, while sensory fibres are relatively more susceptible to ischemia, collateral formation prevents ischemia for quite some time [31].

Direct involvement of the cord may result in inflammatory oedema (myelitis) and rarely it may lead to granuloma formation within the cord [32]. Oedema is seen as hyperintense signal on T2W images with minimal signal alteration on T1W images (Fig. 8.19). Myelitis with a relatively preserved cord associated with fluid collection in the epidural space shows good response to conservative treatment, provided neurological deficit is predominantly due to mechanical compression. However, myelitis associated with granulation tissue with little fluid component as a cause for neurological deficit calls for surgical decompression [33].

Fig. 8.19 Sagittal T2W MR scan shows altered signal in the marrow and intervening disk of lumbar vertebrae. The cord is mildly expanded at this level with T2 hyperintense signal due to cord edema (arrow) –myelitis

8.8 Cord Changes in Chronic Disease

Include myelomalacia, cord atrophy and syringomyelia. Myelomalacia is seen as hyperintense signal on T2w images with a T1 hypointense signal (higher than that of CSF) and may be associated with thinning of the cord. A syrinx is a well-defined tubular, fluid-filled region (showing CSF signal characteristics) within the spinal cord which is usually tapered to one or both ends and can be septated (Fig. 8.20). It is associated with poor neurological outcomes, [32, 34] however, mild atrophy of the cord can still be compatible with successful neurological outcomes.

Paraplegia may occur even with healed disease due to a residual severe deformity, even after many years. It is produced either due to stretching of the spinal cord over internal bony deformity, with resultant gliosis, or due to dural scarring causing constriction of cord [33].

Fig. 8.20 Sagittal T2 weighted MRI scan in an old TB spine at C5/6 level post decompression shows residual deformity in the form of reversal of normal cervical lordosis and thinning of the cord at the same level (arrow). An elongated tubular structure showing CSF like signal within the spinal cord from C2 to C3 level (asterix)–syrinx formation

8.9 Atypical Spinal Tuberculosis: [5, 35]

The common paradiscal lesion is readily diagnosed and treated. Atypical spinal tuberculosis can be defined as compressive myelopathy with no visible spinal deformity with the absence of the radiological appearance of a typical vertebral lesion. Such lesions are rare, however, it is crucial that they are not missed as late diagnosis may lead to more chances of complications. Atypical lesions include: single vertebral disease (Fig. 8.8), ivory vertebra, isolated involvement of the neural arch (Fig. 8.18), circumferential vertebral involvement, multifocal vertebral disease, skipped lesion (Fig. 8.1).

Patients with tubercular granulomas in the intradural, epidural or intramedullary spaces may have symptoms of compressive myelopathy, radiculopathy or both, without any obvious spinal deformity or radiological signs, which is also described

Fig. 8.21 Sagittal T1 weighted post contrast through the lumbosacral region reveals thick dural around the distal visualized cord (arrow) and enhancement around the adherent roots(short arrow)-arachnoiditis

as 'spinal tumor syndrome'. Final diagnosis in such conditions is usually made at surgery or histopathological evaluation.

Extraosseous extradural granuloma is when an extradural granulomatous lesion is seen in the absence of bone involvement. Hematogenous dissemination is the likely cause. This manifestation is more common in the dorsal epidural space and in the thoracic segment of spine. Clinically patients present with compressive radiculomyelopathy. On pathologic examination, a granulomatous reaction is found encircling and causing compression of the spinal cord or cauda equina. These findings are well evident on MRI as T1 isointense (relative to the cord) and T2 mixed signal intensity lesions showing homogenous enhancement [36]. Extradural abscess may occur either as primary lesions or may be seen associated with myelitis, arachnoiditis (Fig. 8.21), intramedullary tuberculoma etc. [37]

8.10 Post-Treatment Follow Up

8.10.1 Conventional Radiograph

When the disease is diagnosed at an early stage and treated promptly, healing process may result in complete resolution of radiological findings except for a decreased disc space. Radiological evidence of healing lags behind the clinical features of healing by about 3 months [38].

Moreover, bone destruction or loss of vertebral height and soft tissue paravertebral masses may progress for months while on treatment, however, this should not necessarily be considered as a sign of failed treatment [39].

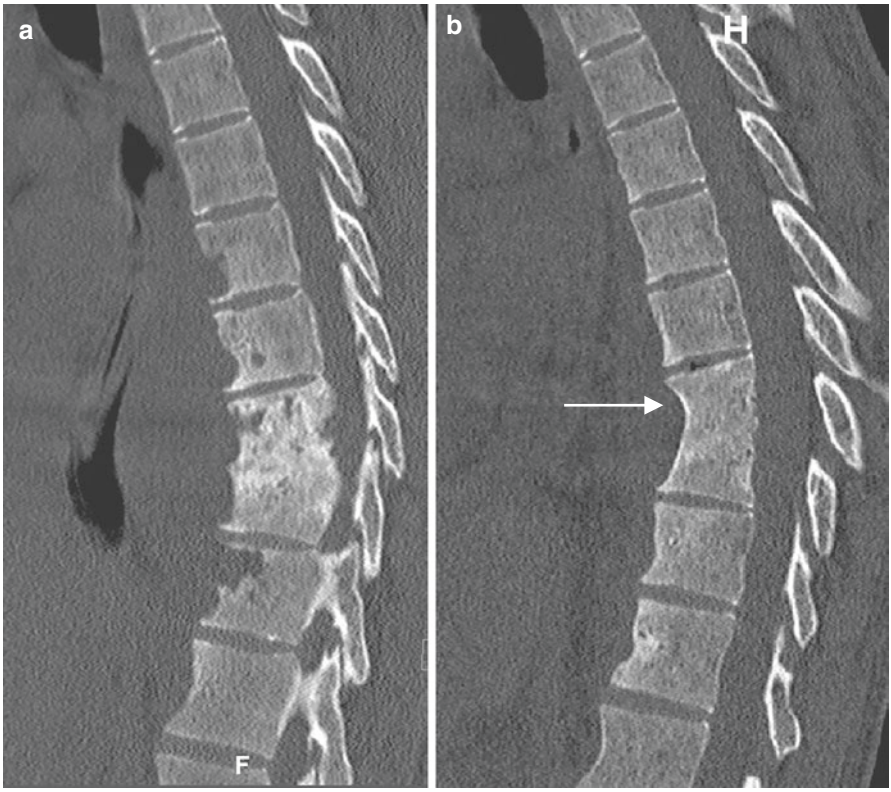

Fig. 8.22 Sagittal CT dorsolumbar spine of a patient with Potts spine before and after treatment. (**a**) Multiple contiguous vertebral destruction with a large prevertebral abscess (**b**) post treatment there is reduction in the prevertebral abscess with bony ankylosis(arrow) of D9 and D10 vertebral bodies, there is regeneration of the D7,8 and D11 vertebral bodies with mild sclerotic reaction.

Early signs of healing on radiology include sharpening of the irregular endplate margins, reappearance and mineralization of the trabeculae which were absorbed earlier. In the early stage of healing, a sclerotic reaction to the diseased bone may give rise to an 'ivory vertebra' i.e. diffuse increase in density of vertebral body [5]. Modern antitubercular drugs result in significant regeneration of the destroyed vertebrae as seen on radiology. Healing by fibrous ankylosis usually occurs when several vertebrae are destroyed with a large gap. Uncommonly, if the disc is completely destroyed with obliteration of the disc space due to collapse and apposition of the vertebrae, healing may take place by bony ankylosis or bone-block formation [1] (Fig. 8.22).

8.11 MRI

Decrease in the size of paraspinal soft issue involvement is the earliest sign of healing. It must be noted, however, that persistence of bone destruction with an altered signal intensity on MRI does not necessarily indicate failed treatment. T1 non-fat saturated images are crucial in follow up, a high T1 signal at the rim of the osseous lesion is an MRI sign of healing. This sequential increase in T1 signal can be followed up in post-treatment imaging as it is found to correlate with clinical healing as well. Besides the non-contrast T1 non-fat suppressed images, T1 fat-suppressed post-contrast images may also reveal reduction in enhancement with healing. Again, the persistence or mild increase in enhancement does not necessarily indicate a failed treatment. MRI also has a role in detection of reactivation of old healed tubercular disease, it is seen as appearance of high signal on T2 images in areas that had turned hypointense during healing. Rarely reactivation may be in the form of an isolated paraspinal collection without osseous involvement. It must be stressed, however, that MRI alone cannot determine disease healing and termination of treatment must be considered only after correlation with clinical and laboratory findings [40].

8.12 Differential Diagnosis

1. Degenerative Spondylosis:
   T2 signal and contrast study can help differentiate the two. The degenerated disc appears T2 hypointense and shows occasional faint enhancement, while the infected disc appears T2 hyperintense and shows strong enhancement [41].
2. Pyogenic Infection: It is often difficult to differentiate the two, however, certain features that favour the diagnosis of tubercular aetiology rather than pyogenic are; Osteoporotic changes with lack of reactive sclerosis on X-ray, late involvement of the intervertebral disc, presence of multiple contiguous vertebral disease

with subligamentous spread, disproportionately large paraspinal abscess showing calcification, neural arch involvement and skip lesions [41, 42].
3. Brucellosis: Intradiscal gas, minimal paraspinal soft tissue involvement with lower lumbar predilection are ommon.
4. Sarcoidosis: It is the great masquerader; hence it may occasionally be identical to tuberculous involvement of multiple vertebrae [42].
5. Others: In case of single vertebral involvement due to metastatic disease or eosinophilic granuloma, differentiation from tubercular disease could be done by observing the disc involvement and paraspinal soft tissue with/without calcification. Other differential diagnosis that an involve consecutive vertebral bodies involvement include lymphoma, multiple myeloma, chordoma. [22, 42, 43].

References

1. Kumar K. Spinal tuberculosis, natural history of disease, classifications and principles of management with historical perspective. Eur J Orthop Surg Traumatol Orthop Traumatol. 2016 Aug;26(6):551–8.
2. Rajasekaran S, Soundararajan DCR, Shetty AP, Kanna RM. Spinal Tuberculosis: Current Concepts. Glob Spine J. 2018 Dec;8(4 Suppl):96S–108S.
3. Hodgson AR, Stock FE, Fang HSY, Ong GB. Anterior spinal fusion the operative approach and pathological findings in 412 patients with pott's disease of the spine. Br J Surg. 1960 Sep;48(208):172–8.
4. Agrawal V, Patgaonkar P, Nagariya S. Tuberculosis of spine. J Craniovertebral Junction Spine. 2010;1(2):74.
5. Pande KC, Babhulkar SS. Atypical Spinal Tuberculosis. Clin Orthop. 2002 May;398:67–74.
6. Ansari S, Amanullah MF, Rauniyar R, Ahmad K. Pott′s spine: Diagnostic imaging modalities and technology advancements. North. Am J Med Sci. 2013;5(7):404.
7. Garg RK, Somvanshi DS. Spinal tuberculosis: A review. J Spinal Cord Med. 2011 Sep;34(5):440–54.
8. V A, Pr P, Sp N. Tuberculosis of spine [Internet]. Vol. 1, Journal of craniovertebral junction & spine. J Craniovertebr Junction Spine; 2010 [cited 2020 Dec 3]. Available from: https://pubmed.ncbi.nlm.nih.gov/21572628/
9. Bhargava SK, Gupta S. Large retropharyngeal cold abscess in an adult with respiratory distress. J Laryngol Otol. 1990 Feb;104(2):157–8.
10. Boachie-Adjei O, Squillante RG. Tuberculosis of the spine. Orthop Clin North Am. 1996 Jan;27(1):95–103.
11. Rivas-Garcia A, Sarria-Estrada S, Torrents-Odin C, Casas-Gomila L, Franquet E. Imaging findings of Pott's disease. Eur Spine J. 2013 Jun;22(Suppl 4):567–78.
12. Kukreja R, Mital M, Gupta PK. Evaluation of Spinal Tuberculosis by Plain X-Rays and Magnetic Resonance Imaging in a Tertiary Care Hospital in Northern India. A Prospective Study. 2018;5(2):6.
13. Jain AK. Tuberculosis of the skeletal system. Indian J Orthop. 2016;50(3):337.
14. Sagane SS, Patil VS, Bartakke GD, Kale KY. Assessment of Clinical and Radiological Parameters in Spinal Tuberculosis: Comparison between Human Immunodeficiency Virus-Positive and Human Immunodeficiency Virus-Negative Patients. Asian Spine J. 2020 Dec 31;14(6):857–63.

15. Kumar K. Posterior Spinal Tuberculosis: A Review. Mycobact Dis [Internet]. 2017; [cited 2020 Dec 27];07(02). Available from: https://www.omicsonline.org/open-access/posterior-spinal-tuberculosis-a-review-2161-1068-1000243.php?aid=90703
16. Abdelwahab IF, Camins MB, Hermann G, Klein MJ. Vertebral arch or posterior spinal tuberculosis. Skelet Radiol. 1997 Dec 9;26(12):737–40.
17. Kumar K. A clinical study and classification of posterior spinal tuberculosis. Int Orthop. 1985 Nov;9(3):147–52.
18. Department of Radiology, Nagpur NKPSIMS, Patil DS. Assessment of imaging finding in Spinal tuberculosis. J Med Sci Clin Res [Internet]. 2019; Jan 20 [cited 2020 Dec 31];7(1). Available from: http://jmscr.igmpublication.org/v7-i1/93%20jmscr.pdf
19. Moon M-S. Tuberculosis of Spine: Current Views in Diagnosis and Management. Asian Spine J. 2014;8(1):97.
20. Rasouli MR, Mirkoohi M, Vaccaro AR, Yarandi KK, Rahimi-Movaghar V. Spinal Tuberculosis: Diagnosis and Management. Asian Spine J. 2012 Dec;6(4):294–308.
21. Harisinghani MG, McLoud TC, Shepard J-AO, Ko JP, Shroff MM, Mueller PR. Tuberculosis from Head to Toe. Radiographics. 2000 Mar 1;20(2):449–70.
22. Sharif HS, Morgan JL, al Shahed MS, al Thagafi MY. Role of CT and MR imaging in the management of tuberculous spondylitis. Radiol Clin N Am. 1995 Jul;33(4):787–804.
23. Gouliamos AD, Kehagias DT, Lahanis S, Athanassopoulou AA, Moulopoulou ES, Kalovidouris AA, et al. MR imaging of tuberculous vertebral osteomyelitis: pictorial review. Eur Radiol. 2001;11(4):575–9.
24. Hong SH, Choi J-Y, Lee JW, Kim NR, Choi J-A, Kang HS. MR Imaging Assessment of the Spine: Infection or an Imitation? Radiographics. 2009 Mar 1;29(2):599–612.
25. Danchaivijitr N, Temram S, Thepmongkhol K, Chiewvit P. Diagnostic accuracy of MR imaging in tuberculous spondylitis. J Med Assoc Thail Chotmaihet Thangphaet. 2007 Aug;90(8):1581–9.
26. Corea JR, Tamimi TM. Tuberculosis of the Arch of the Atlas: Case Report. Spine. 1987 Aug;12(6):608–11.
27. Rao BD, Rao KS, Subrhamanian MV, Reddy MV. Granulomatous lesions of the spinal epidural space. Neurol India. 1965 Sep;13(3):89–92.
28. Kocen RS, Parsons M. NEUROLOGICAL COMPLICATIONS OF TUBERCULOSIS: SOME UNUSUAL MANIFESTATIONS. QJM Int J Med. 1970 Jan 1;39(1):17–30.
29. Kak VK, Pani KC, Chopra JS. Epidural spinal tuberculoma presenting as 'spinal tumour syndrome'. Tubercle. 1972 Jun 1;53(2):139–42.
30. Solomon A, Sacks AJ, Goldschmidt RP. Neural arch tuberculosis: a morbid disease. Radiographic and computed tomographic findings. Int Orthop. 1995;19(2):110–5.
31. Bosworth DM, Della Pietra A, Rahilly G. PARAPLEGIA RESULTING FROM TUBERCULOSIS OF THE SPINE. JBJS. 1953 Jul;35(3):735–40.
32. Kumar R. Spinal tuberculosis: with reference to the children of northern India. Childs Nerv Syst ChNS Off J Int Soc Pediatr Neurosurg. 2005 Jan;21(1):19–26.
33. Negi SS, Khan SFB, Gupta S, Pasha ST, Khare S, Lal S. Comparison of the conventional diagnostic modalities, bactec culture and polymerase chain reaction test for diagnosis of tuberculosis. Indian J Med Microbiol. 2005 Jan;23(1):29–33.
34. Andronikou S, Bindapersad M, Govender N, Waner JI, Segwe A, Palliam S, et al. Musculoskeletal tuberculosis - imaging using low-end and advanced modalities for developing and developed countries. Acta Radiol Stockh Swed 1987. 2011 May 1;52(4):430–41.
35. JaypeeDigital | Tuberculosis of the Spine [Internet]. [cited 2021 Jan 12]. Available from: https://www.jaypeedigital.com/book/9789350258835/chapter/ch7
36. Hsu LC, Leong JC. Tuberculosis of the lower cervical spine (C2 to C7). A report on 40 cases. J Bone Joint Surg Br. 1984 Jan;66(1):1–5.
37. Trivedi R, Saksena S, Gupta RK. Magnetic resonance imaging in central nervous system tuberculosis. Indian J Radiol Imaging. 2009 Jan 10;19(4):256.

38. Jaypee Brothers: Book Details [Internet]. [cited 2020 Dec 27]. Available from: https://www.jaypeebrothers.com/pgDetails.aspx?cat=s&book_id=9788194709022
39. Boxer DI, Pratt C, Hine AL, McNicol M. Radiological features during and following treatment of spinal tuberculosis. Br J Radiol. 1992 Jun 1;65(774):476–9.
40. Le Page L, Feydy A, Rillardon L, Dufour V, Le Hénanff A, Tubach F, et al. Spinal tuberculosis: a longitudinal study with clinical, laboratory, and imaging outcomes. Semin Arthritis Rheum. 2006 Oct;36(2):124–9.
41. Sharif HS, Aideyan OA, Clark DC, Madkour MM, Aabed MY, Mattsson TA, et al. Brucellar and tuberculous spondylitis: comparative imaging features. Radiology. 1989 May;171(2):419–25.
42. Yao DC, Sartoris DJ. Musculoskeletal tuberculosis. Radiol Clin N Am. 1995 Jul;33(4):679–89.
43. Moore SL, Rafii M. Imaging of musculoskeletal and spinal tuberculosis. Radiol Clin N Am. 2001 Mar;39(2):329–42.